Identification of the Limiting Species in the Plutonium(IV) Carbonate System. Solid State and Solution Molecular Structure of the $[Pu(CO_3)_5]^{6-}$ Ion

David L. Clark,*,[1a] Steven D. Conradson,[1b] D. Webster Keogh,[1c] Phillip D. Palmer,[1c] Brian L. Scott,[1d] and C. Drew Tait[1c]

Chemical Science and Technology, Materials Science and Technology, and Nuclear Materials Technology Divisions, Los Alamos National Laboratory, Los Alamos, New Mexico 87545, and the Seaborg Institute for Transactinium Science, Los Alamos, New Mexico 87545

Received September 18, 1997

The identity of the limiting Pu(IV) species under high carbonate concentrations has been determined to be $Pu(CO_3)_5^{6-}$. Single crystals of $[Na_6Pu(CO_3)_5]_2{\cdot}Na_2CO_3{\cdot}33H_2O$ were obtained from a 0.15 M solution of Pu(IV) in 2.6M Na_2CO_3. The asymmetric unit contains a complex network consisting of $[Pu(CO_3)_5]^{6-}$ anions and Na^+ cations which are linked through interactions with CO_3^{2-} and H_2O ligands. Each Na^+ ion is coordinated to the O atoms of H_2O or CO_3^{2-} ligands such that the Na^+ ions achieve either octahedral or square-based pyramidal coordination. The $[Pu(CO_3)_5]^{6-}$ anion can be viewed as a pseudohexagonal bipyramid with three CO_3^{2-} ligands in a equatorial plane and two in axial positions. EXAFS data for Pu(IV) in 2.5M Na_2CO_3 solution were collected at the Pu L_{III} edge. Curve fitting reveals three shells in the FT spectrum. The first shell contains ten O atoms with Pu−O = 2.42(2) Å; the second shell was fit with five C atoms with Pu- - -C = 2.89(2) Å; and the third shell was fit with five O atoms with Pu- - -O = 4.17(2) Å. These distances and coordination numbers correspond well with the average Pu−O, nonbonding Pu- - -C, and distal Pu- - -O distances of 2.415(7), 2.874(9), and 4.117(10) Å, respectively, found in the $[Pu(CO_3)_5]^{6-}$ ion in the solid-state structure of $[Na_6Pu(CO_3)_5]_2{\cdot}Na_2CO_3{\cdot}33H_2O$. The UV−vis diffuse reflectance spectrum of a single crystal of $[Na_6Pu(CO_3)_5]_2{\cdot}Na_2CO_3{\cdot}33H_2O$ ground into a powder is nearly identical to the solution absorption spectrum of the limiting Pu(IV) carbonato complex in 2.5 M Na_2CO_3 solution. The peak by peak correspondence by position and relative absorption strengths, along with solution EXAFS data, suggest that the Pu(IV) chromophore is the same in both cases, and confirms that the $[Pu(CO_3)_5]^{6-}$ ion is the limiting species in high carbonate solutions. Crystal data for $[Na_6Pu(CO_3)_5]_2{\cdot}Na_2CO_3{\cdot}33H_2O$: monoclinic space group $P2_1/c$ (No. 14), a = 9.860(2) Å, b = 17.427(2) Å, c = 18.210(1) Å, β = 101.42(1)°, Z = 2, R_1 = 0.0337, wR_2 = 0.0775.

Introduction

The carbonate anion is a common ligand in nearly all natural water environments, and carbonate complexation in aqueous solution is known to affect the solubilities of actinide ions through formation of anionic complexes.[2−5] This is especially true for the tetravalent plutonium ion, which forms strong complexes with hard oxygen donor ligands. Over the past decade, there have been many studies focused on determination of the identities of the chemical species present in the plutonium(IV) carbonate system.[2,3,6−13] While there is a fair amount of scatter in the Pu(IV) carbonate formation constants, there are essentially two interpretations of Pu(IV) carbonate thermodynamic data in the literature. One interpretation[6−10] favors the simple stepwise formation of $[Pu(CO_3)_n]^{4-2n}$ complexes (n = 0−5, eq 1) while the other[11−13] favors the formation of mixed hydroxo−carbonato complexes of general formula $[Pu(OH)_m(CO_3)_n]^{4-m-2n}$ (eq 2). The difficulty in interpretation

$$Pu^{4+}(aq) + nCO_3^{2-} \rightleftarrows [Pu(CO_3)_n]^{4-2n} \quad (n = 1, 2, 3, 4, 5) \tag{1}$$

$$Pu^{4+}(aq) + nCO_3^{2-} + mOH^- \rightleftarrows [Pu(OH)_m(CO_3)_n]^{4-m-2n} \tag{2}$$

$$[Pu(CO_3)_5]^{6-} \rightleftarrows [Pu(CO_3)_4]^{4-} + CO_3^{2-} \tag{3}$$

of the data arises from the fact that the hydrolysis and carbonate formation constants are similar in magnitude, making it difficult to distinguish between the various models. As a result, it is important to unequivocally identify the nature of the limiting complex in the plutonium carbonate system to provide a starting

(1) (a) Mail Stop E500. (b) Mail Stop D429. (c) Mail Stop G739. (d) Mail Stop J514.
(2) Clark, D. L.; Hobart, D. E.; Neu, M. P. *Chem. Rev.* **1995**, *95*, 25.
(3) Fuger, J. *Radiochim. Acta* **1992**, *59*, 81.
(4) Dozol, M.; Hagemann, R. *Pure Appl. Chem.* **1993**, *65*, 1081.
(5) Silva, R. J.; Nitsche, H. *Radiochim. Acta* **1995**, *70/71*, 3776.
(6) Kim, J. I.; Lierse, C.; Baumgartner, F. In *ACS Symposium Series*; American Chemical Society: Washington, DC, 1983; No. 216, p 317.
(7) Nitsche, H.; Silva, R. J. *Radiochim. Acta* **1996**, *72*, 65.
(8) Eiswirth, M.; Kim, J. I.; Lierse, C. *Radiochim. Acta* **1985**, *38*, 1971.
(9) Capdevila, H.; Vitorge, P.; Giffaut, E.; Delmau, L. *Radiochim. Acta* **1996**, 93.
(10) Lierse, C.; Kim, J. I. *RCM 02286*; Institut fur Radiochemie: TU München, 1986.
(11) Hobart, D. E.; Palmer, P. D.; Newton, T. W. *The carbonate complexation of plutonium(IV)*; Report LA-UR-86-968, Los Alamos National Laboratory: Los Alamos, NM, 1986.
(12) Tait, C. D.; Ekberg, S. A.; Palmer, P. D.; Morris, D. E. *Plutonium carbonate speciation changes as measured in dilute solutions with photoacoustic spectroscopy*; Report LA-12886-MS; Los Alamos National Laboratory: Los Alamos, NM, 1995.
(13) Yamaguchi, T.; Sakamoto, Y.; Ohnuki, T. *Radiochim. Acta* **1994**, *66/67*, 9.

S0020-1669(97)01190-7 CCC: $15.00
Published on Web 06/15/1998

point for identification of the other complexes formed in the equilibria. This approach was recently utilized by Capdevila et al.,[9] who studied the dissociation of the limiting complex and interpreted their data in terms of the equilibria between a limiting $[Pu(CO_3)_5]^{6-}$ complex and $[Pu(CO_3)_4]^{4-}$ as indicated in eq 3. Their interpretation hinges on the assumption that the limiting complex is $[Pu(CO_3)_5]^{6-}$, for which there has been no definitive proof. This assumption was justified by analogy to the formation of other tetravalent f-element pentacarbonato complexes, primarily with Th(IV)[14−16] but also with U(IV),[17,18] Am(IV),[19,20] and Ce(IV).[14,15] Conclusive evidence for these complexes exists only for Th(IV), for which there are X-ray crystal structures for $M_6Th(CO_3)_5{\cdot}nH_2O$ (M = Na,[15] $n = 12$; M = $C(NH_2)_3^+$,[14,21] $n = 4$), and solubility[22,23] and EXAFS[23] experiments which imply the same species in solution.[16] Solid Pu(IV) carbonato complexes of general formula $M_{(2n-4)}Pu(CO_3)_n{\cdot}mH_2O$ (M = Na^+, K^+, NH_4^+; $n = 4$, 5, 6, 8),[24] $(NH_4)_4Pu(CO_3)_4{\cdot}4H_2O$ and $[Co(NH_3)_6]_2Pu(CO_3)_5{\cdot}5H_2O$, have been reported;[25] however, there is little characterizing data on these solids, making it difficult to evaluate these reports. While there is a great deal of qualitative information regarding anionic carbonate complexes of Pu(IV), reliable quantitative data are rare. No direct evidence has been presented for the existence of $[Pu(CO_3)_5]^{6-}$, and a determination of the formulation of the highly soluble limiting species generated at high carbonate concentration would be a first step to resolving this uncertainty. We report here our experiments to determine unequivocally the nature of the Pu(IV) carbonate-limiting species, both in the solid state and in solution.

Results and Discussion

Synthesis and Species Corroboration. The study of plutonium(IV) carbonato complexes poses experimental challenges due to the strong tendency for Pu(IV) solutions to undergo hydrolysis and polymerization reactions, and pervasive α-particle self-irradiation that affects the Pu redox state in solution.[26] The consequences of radiolysis on plutonium-containing solutions can be reduced by using ^{242}Pu, which is approximately 16 times less radioactive than the more common ^{239}Pu isotope. $^{242}PuO_2$ was dissolved in concentrated $HClO_4$ and heated to fuming in order to oxidize all Pu to the VI state. The oxidation state was then adjusted to Pu(IV), and the solution was purified using anion exchange chromatography (see Experimental Section). A small aliquot of purified $^{242}Pu^{4+}$(aq) was taken from an acidic stock solution and added to 3.0 M Na_2CO_3 solution. The volume of acid added was sufficient to bring the overall CO_3^{2-} concentration to 2.6 M. It is important that the preparation be carried out in this manner in order to avoid competing hydrolysis side reactions. The resulting green solution was characterized using UV−vis−NIR spectroscopy. The absorption spectrum showed peaks characteristic of the limiting Pu(IV) complex (i.e. 485.5 nm) as reported by others.[8,9,11]

Table 1. Crystal Data and Structure Refinement for $[Na_6Pu(CO_3)_5]_2{\cdot}Na_2CO_3{\cdot}33H_2O$

empirical formula	$C_{11}H_{66}Na_{14}O_{66}Pu_2$
fw	2060.50
T, K	293(2)
crystal dimens	0.16 × 0.25 × 0.33 mm
wavelength, Å	0.71073
space group	$P2_1/c$
unit cell dimensions	
a, Å	9.860(2)
b, Å	17.427(2)
c, Å	18.210(1)
β, deg	101.42
V, Å^3	3067.1(7)
Z	2
D_{calc}, g cm^{-3}	2.231
μ, mm^{-1}	2.369
$\theta_{max}/\theta_{min}$	0.778/0.725
F(000)	2004
theta range, deg	2.6−22.5
no. of reflcns collcd	5189
no. of indep reflcns	3995 [*R*(int) = 0.0356]
no. of data/restraints/params	3995/0/433
goodness-of-fit on F^2	1.054
final *R* indices [$I > 2\sigma(I)$][a]	$R_1 = 0.0337$, $wR_2 = 0.0775$
R indices (all data)	$R_1 = 0.0524$, $wR_2 = 0.0850$
largest diff. peak and hole, e Å^{-3}	0.696 and −0.863

[a] $R_1 = \sum||F_o|-|F_c||/\sum|F_o|$; $wR_2 = [\sum[w(F_o^2 - F_c^2)^2]/\sum[w(F_o^2)^2]]^{1/2}$; and $w = 1/[\sigma^2(F_o^2) + (0.0397P)^2 + 5.0273P]$.

Table 2. Selected Bond Lengths (Å) and Angles (deg) for $[Na_6Pu(CO_3)_5]_2{\cdot}Na_2CO_3{\cdot}33H_2O$

Pu(1)−O(1)	2.418(5)	Pu(1)−C(1)	2.867(9)
Pu(1)−O(2)	2.415(6)	Pu(1)−C(2)	2.854(8)
Pu(1)−O(4)	2.381(6)	Pu(1)−C(3)	2.881(9)
Pu(1)−O(5)	2.420(6)	Pu(1)−C(4)	2.896(9)
Pu(1)−O(7)	2.415(6)	Pu(1)−C(5)	2.873(8)
Pu(1)−O(8)	2.412(5)	Pu(1)−O(3)	4.121(9)
Pu(1)−O(10)	2.430(6)	Pu(1)−O(6)	4.088(10)
Pu(1)−O(11)	2.413(7	Pu(1)−O(9)	4.113(10)
Pu(1)−O(14)	2.418(7)	Pu(1)−O(12)	4.141(10)
Pu(1)−O(13)	2.423(7)	Pu(1)−O(15)	4.128(10)
O(1)−Pu(1)−O(8)	68.1(2)	O(10)−Pu(1)−O(13)	144.3(2)
O(2)−Pu(1)−O(4)	68.5(2)	O(10)−Pu(1)−O(14)	146.4(3)
O(5)−Pu(1)−O(7)	73.7(2)	O(11)−Pu(1)−O(13)	144.6(3)
O(1)−Pu(1)−O(2)	53.1(2)	O(11)−Pu(1)−O(14)	141.3(3)
O(4)−Pu(1)−O(5)	51.7(2)	O(1)−C(1)−O(2)	113.6(8)
O(7)−Pu(1)−O(8)	53.2(2)	O(4)−C(2)−O(5)	111.9(7)
O(10)−Pu(1)−O(11)	52.4(2)	O(7)−C(3)−O(8)	112.2(7)
O(13)−Pu(1)−O(14)	50.8(2)	O(10)−C(4)−O(11)	111.8(8)
		O(13)−C(5)−O(14)	113.0(8)

Solid-State and Solution Molecular Structure

Single-Crystal X-ray Diffraction. Single crystals of $[Na_6Pu(CO_3)_5]_2{\cdot}Na_2CO_3{\cdot}33H_2O$ were prepared by allowing a 0.15 M solution of Pu(IV) in 2.6 M Na_2CO_3 to stand undisturbed for several months, during which time large green cubes were deposited. The data collection and crystallographic parameters are summarized in Table 1, and the selected interatomic distances and angles are given in Table 2. A thermal ellipsoid drawing of the central $[Pu(CO_3)_5]^{6-}$ anion is shown in Figure

(14) Voliotis, P. S.; Rimsky, E. A. *Acta Crystallogr.* **1975**, *B31*, 2612.
(15) Voliotis, P. S.; Rimsky, E. A. *Acta Crystallogr.* **1975**, *B31*, 2615.
(16) Dervin, J.; Faucherre, J. *Bull. Soc. Chim. Fr.* **1973**, *11*, 2930.
(17) Ciavatta, L.; Ferri, D.; Grenthe, I.; Salvatore, F.; Spahiu, K. *Inorg. Chem.* **1983**, *22*, 2088.
(18) Grenthe, I.; Fuger, J.; Konigs, R. J. M.; Lemire, R. J.; Muller, A. B.; Nguyen-Trung, C.; Wanner, H. *Chemical thermodynamics of uranium*; Elsevier Science Publishing Company, Inc.: New York, 1992; Vol. 1.
(19) Robouch, P. Ph.D. Thesis, Ecole Europenne des Hautes Etudes des Industries Chimiques de Strasbourg, France, 1989.
(20) Silva, R. J.; Bidoglio, G.; Rad, M. H.; Robouch, P.; Waner, H.; Puigdomenech, I. *NEA-TDB: Chemical thermodynamics of americium*; Elsevier Science Publishers: New York, 1995.
(21) Marsh, R. E.; Herbstein, F. H. *Acta Crystallogr.* **1988**, *B44*, 77.
(22) Oesthols, E.; Bruno, J.; Grenthe, I. *Geochim. Cosmochim. Acta* **1994**, *58*, 613.
(23) Felmy, A. R.; Rai, D.; Sterner, S. M.; Mason, M. J.; Hess, N. J.; Conradson, S. D. *J. Sol. Chem.* **1997**, *26*, 233.
(24) Gel'man, A. D.; Zaitsev, L. M. *Zh. Neorg. Khim.* **1958**, *3*, 1304.
(25) Ueno, K.; Hoshi, M. *J. Inorg. Nucl. Chem.* **1970**, *32*, 3817.
(26) Katz, J. J.; Seaborg, G. T.; Morss, L. R. *The chemistry of the actinide elements*; Chapman and Hall: London, 1986.

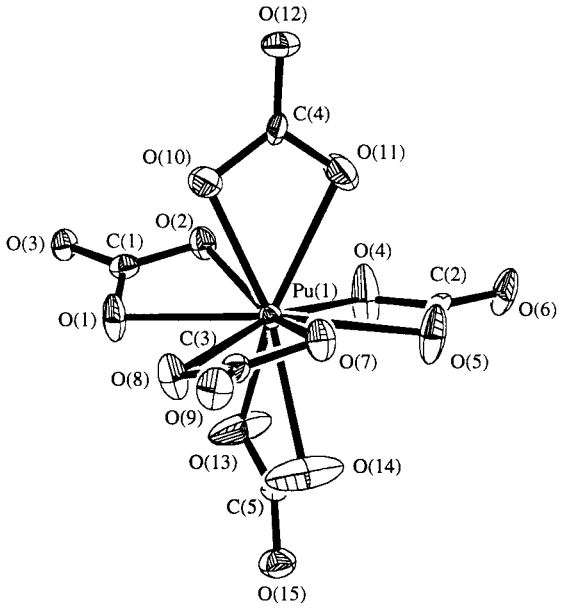

Figure 1. Thermal ellipsoid plot (50% probability) of the central $[Pu(CO_3)_5]^{6-}$ ion, emphasizing the pseudohexagonal bipyramidal coordination geometry and giving the atom number scheme used in the tables. Carbonate ligands containing C(1), C(2), and C(3) lie in the "equatorial" plane.

1, and a ball-and-stick drawing illustrating the secondary coordination environment of Na and O atoms surrounding the central $[Pu(CO_3)_5]^{6-}$ ion and providing the atom-numbering scheme used in the tables is shown in Figure 2.

The asymmetric unit contains a complex network consisting of $[Pu(CO_3)_5]^{6-}$ anions and Na^+ cations which are linked through shared interactions with carbonate and water ligands. There is one disordered lattice carbonate ligand lying near the inversion center. Carbonate ligands interact with both Pu^{4+} and Na^+ ions, while water ligands are only bound to Na^+ ions. Each Na^+ ion is coordinated to the O atoms of water or carbonate ligands such that the Na^+ ions achieve either octahedral or square-based pyramidal coordination.

The $[Pu(CO_3)_5]^{6-}$ anion consists of a central Pu atom coordinated to ten O atoms of five bidentate carbonato ligands, in a structural unit that is very similar to the related $[Th(CO_3)_5]^{6-}$ anion found in the solid-state structures of $Na_6[Th(CO_3)_5]\cdot 12H_2O$[15] and $[C(NH_2)_3]_6[Th(CO_3)_5]\cdot 4H_2O$.[14,21] While the Th analogue has been described as an irregular decahexahedron,[15] we prefer to view this complex structure as a modification of the well-known hexagonal bipyramidal coordination polyhedron seen in $[AnO_2(CO_3)_3]^{4-}$ complexes.[27−29] This analogy between $[PuO_2(CO_3)_3]^{4-}$ and $[Pu(CO_3)_5]^{6-}$ is illustrated in **I** and **II** below.

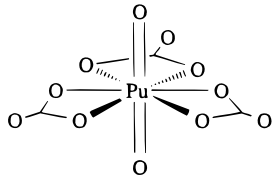

I

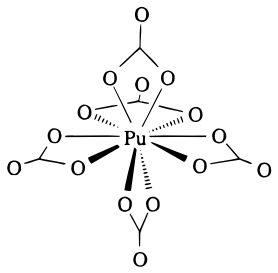

II

Viewed in this way, the $[Pu(CO_3)_5]^{6-}$ ion has three bidentate carbonate ligands in an approximately hexagonal plane and two trans bidentate carbonate ligands occupying pseudoaxial positions as illustrated in Figure 1. These "axial" carbonate ligands are oriented such that the "axial" planes defined by two carbonate ligands are rotated with respect to each other by approximately 90°. The distortions in the three carbonate ligands that occur around the hexagonal equatorial plane are brought about by additional interactions between the coordinated carbonate ligands and the Na^+ ions.

The ten Pu−O distances to the carbonate ligands span a relatively narrow range of 2.381(6)−2.430(6) Å, with an average value of 2.415(7) Å. There are relatively few Pu(IV)−O bond distances to which this value can be compared. The analogous $[Th(CO_3)_5]^{6-}$ ion has average Th−O distances of 2.493(11) Å for the guanidinium salt,[14] and solution EXAFS data determined an average Th−O distance of 2.49 Å.[23] As a result of the actinide contraction, one would expect the Pu(IV)−O distance to be approximately 0.08 Å shorter than the Th(IV)−O distance,[30] for a prediction of 2.41 Å in good agreement with the observed value of 2.42 Å. For comparison, the $[Pu(NO_3)_6]^{2-}$ anion has an average Pu−O distance of 2.49 Å with a higher coordination number of 12,[31] and the analogous $Th(NO_3)_6^{2-}$ ion has an average Th−O distance of 2.57 Å,[32] with a difference of 0.08 Å as expected. Bond distances and angles associated with the carbonate ligands are all within the normal range seen for other actinide carbonate structures.[15,27−29,33] The average C−O distance for all five carbonate ligands is 1.280(10) Å. The O−C−O angles of the carbonate ligand deviate from the ideal value of 120°. The O−C−O angle between O atoms bound to Pu (the bite angle) averages 112.5(8)°, while the remaining two O−C−O angles have opened up somewhat to 123.7(8)°. If one defines the pseudohexagonal plane to contain O(1), O(2), O(4), O(5), O(7), and O(8), then, as in other structures containing three carbonate ligands in a hexagonal plane, the O−Pu−O angles within the hexagonal plane fall into two relatively narrow groupings. The O−Pu−O angles between O atoms of a bidentate carbonate ligand average 52.2(2)°, while O−Pu−O angles between adjacent carbonate ligands average 70.1(2)°. The sum of these angles within the "hexagonal plane" of three carbonate ligands is 368.3(2)°, with the slight out-of-plane distortion due to interactions between carbonate O atoms and adjacent Na atoms resulting in deviation from the expected 360° for a strictly planar arrangement.

A complex network of Na atoms surrounds the "equatorial" plane of the pseudo hexagonal bipyramidal $[Pu(CO_3)_5]^{6-}$ ion. The Na ions interact with either H_2O or CO_3^{2-} ligands to form pentagonal bipyramidal or pseudo-octahedral coordination about each Na ion. Five coordination is found for Na(1) and Na(2), which have average Na−O distances of 2.358(8) and 2.361(8) Å, respectively. Six coordination is found for Na(3) − Na(7), which have longer average Na−O distances of 2.442(8), 2.451(9), 2.418(7), 2.429(8), and 2.444(7) Å, respectively. Remarkably, there are no Na−O interactions to the distal carbonate O atoms, O(12) and O(15) of the "axial" carbonate ligands. These O atoms are nested into a pocket formed by the network of NaO_6 and NaO_5 polyhedra, as seen in the ball-and-stick drawing

(27) Anderson, A.; Chieh, C.; Irish, D. E.; Tong, J. P. K. *Can. J. Chem.* **1980**, *58*, 1651.
(28) Coda, A.; Dell Giusta, A.; Tazzoli, V. *Acta Crystallogr.* **1981**, *B37*, 1496.
(29) Graziani, R.; Bombieri, G.; Forsellini, E. *J. Chem. Soc., Dalton Trans.* **1972**, *19*, 2059.
(30) Shannon, R. D. *Acta Crystallogr. A.* **1976**, *32*, 752.
(31) Allen, P. G.; Veirs, D. K.; Conradson, S. D.; Smith, C. A.; Marsh, S. F. *Inorg. Chem.* **1996**, *35*, 2841.
(32) Rammo, N. N.; Hamid, K. R.; Khaleel, B. A. *J. Less Common Met.* **1990**, *162*, 1.

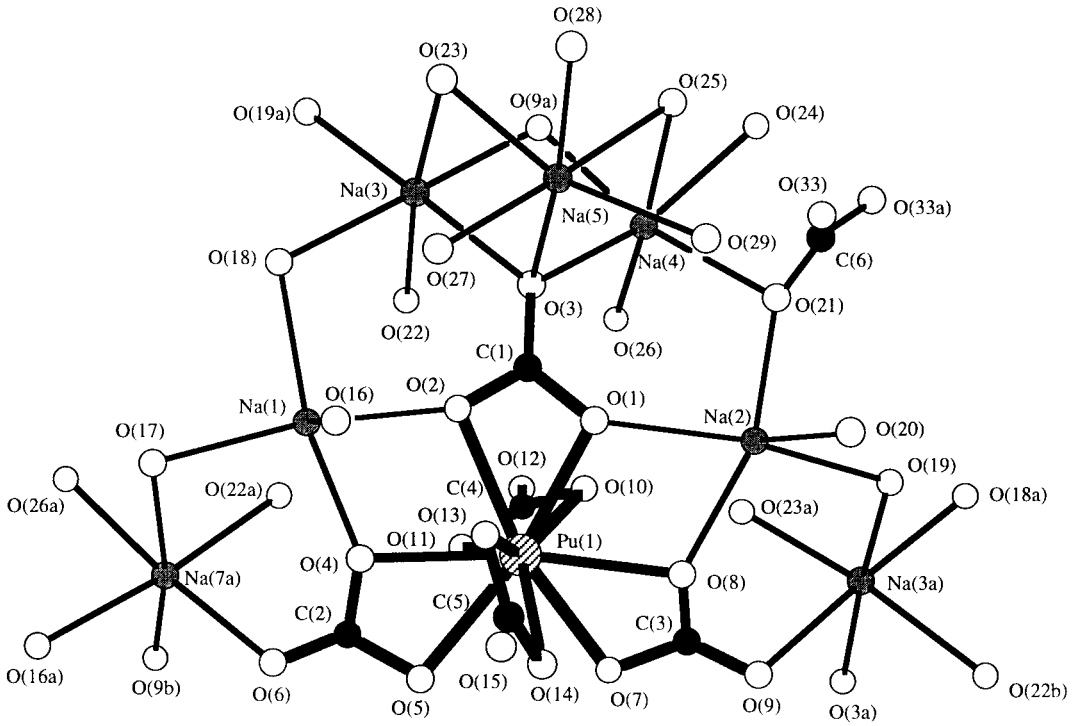

Figure 2. Ball-and-stick drawing of $[Na_6Pu(CO_3)_5]_2 \cdot Na_2CO_3 \cdot 33H_2O$ showing the arrangement of Na^+ and H_2O about the central $[Pu(CO_3)_5]^{6-}$ unit. The carbonate ligand in the lattice, C(6), was modeled with half-occupancy such that O(21) is either part of a carbonate or water molecule.

in Figure 2. The distal O atoms of the "axial" carbonate ligands have short O···O contacts with water molecules averaging 2.759 Å, well within the region expected for H-bonding interactions.[34]

Solution EXAFS Studies. The single-crystal X-ray diffraction studies showed that the $[Pu(CO_3)_5]^{6-}$ ion exists in the solid state but revealed no information regarding the nature of the Pu carbonato complex ion in solution. We turned to extended X-ray absorption fine structure (EXAFS) spectroscopy for structural details of the limiting plutonium(IV) ion in 2.5 M Na_2CO_3 solution. Under these conditions, the limiting Pu(IV) species is characterized by a strong electronic absorption band at 485.5 nm.[8,9,11] Although a small amount of precipitate was noted after the experiment was completed, the X-ray beam was focused on the center of the EXAFS sample cell where only solution species were present. X-ray absorption measurements were performed at the plutonium L_{III} edge. Electronic absorption spectra of the solution from which the EXAFS sample was taken were examined both before and after EXAFS analysis and indicated that the same limiting Pu(IV) species was present in excess of 99%. The background-subtracted k^3-weighted EXAFS spectrum is shown in Figure 3a, where experimental data are shown as a solid line, and the theoretical fit is indicated as a dotted line. The Fourier transform and theoretical fit (without phase corrections) of the k^3-weighted EXAFS data are shown in Figure 3b. Note that because the Fourier transform is not corrected for the EXAFS phase shift, the peak positions do not correspond directly to the bond distance from the central Pu determined by the theoretical fit.

The theoretical EXAFS modeling code, FEFF7,[35,36] of Rehr et al. was employed to calculate the backscattering phases and amplitudes of the individual neighboring atoms, using mono- and bidentate ligation models. The fitting parameters found for the Pu solution structure are listed in Table 3, where the data were fit from $k = 2.288$ to 11.864 $Å^{-1}$. The values for the bond distances and number of atoms in each shell are consistent with the formation of a pentacarbonato Pu(IV) complex quite similar to the species found in the solid state. The goodness of fit can most intuitively be judged by comparing the FT spectrum with the fit, as each shell's contribution can readily be seen. The limiting species in high carbonate solution for Pu(IV) is best fit using five carbonate ligands and hence is consistent with the $[Pu(CO_3)_5]^{6-}$ formulation found in the solid state. The first shell was fit with ten O atoms with a Pu−O distance of 2.41(1) Å, which corresponds remarkably well with the average value of 2.415(7) Å for the $[Pu(CO_3)_5]^{6-}$ ion found in the solid-state structure of $[Na_6Pu(CO_3)_5]_2 \cdot Na_2CO_3 \cdot 33H_2O$. The second shell was fit with five C atoms at a Pu−C distance of 2.88(2) Å, and can be compared with the average nonbonding Pu- - -C distance of 2.874(9) Å found in the solid-state structure. The third shell was best fit by five O atoms at a Pu- - -O distance of 4.16(2) Å and can be compared with the average nonbonding Pu- - -O distance to the distal O atoms of 4.117(10) Å.

To further confirm the number of ligands, the current data were compared with the four different data sets (either aqueous or sorbed onto resins) for the known $[Pu(NO_3)_6]^{2-}$ complex.[31,37] The data for both the $[Pu(CO_3)_n]^{4-2n}$ and $[Pu(NO_3)_6]^{2-}$ were analyzed with identical parameters, i.e., two oxygen shells, one carbon or nitrogen shell, $k = 3-11$, and $S_0^2 = 0.935$, 0.850, and 0.800 for the three shells (O, C/N, O), respectively. Each data set was refined, allowing all parameters to float except the scaling factor, S_0^2. The resulting distances, coordination numbers, and Debye−Waller factor, σ, are given in Table 4. The radial distribution function, RDF, for each of the k^3 fits was determined. The RDF of the first shell for each fit is shown in Figure 4. The intensity of the RDF is linearly dependent on

(33) Allen, P. G.; Bucher, J. J.; Clark, D. L.; Edelstein, N. M.; Ekberg, S. A.; Gohdes, J. W.; Hudson, E. A.; Kaltsoyannis, N.; Lukens, W. W.; Neu, M. P.; Palmer, P. D.; Reich, T.; Shuh, D. K.; Tait, C. D.; Zwick, B. D. *Inorg. Chem.* **1995**, *34*, 4797.
(34) Pauling, L. *The nature of the chemical bond*, 3rd ed.; Cornell University Press: Ithaca, NY, 1960; p 644.
(35) Ankudinov, A. L. Ph.D. Thesis, University of Washington, 1996.
(36) Ankudinov, A. L.; Rehr, J. J. *Phys. Rev. B* **1997**, *56*, R1712.
(37) Veirs, D. K.; Smith, C. A.; Berg, J. M.; Zwick, B. D.; Marsh, S. F.; Allen, P.; Conradson, S. D. *J. Alloys Compd.* **1996**, *213/214*, 328.

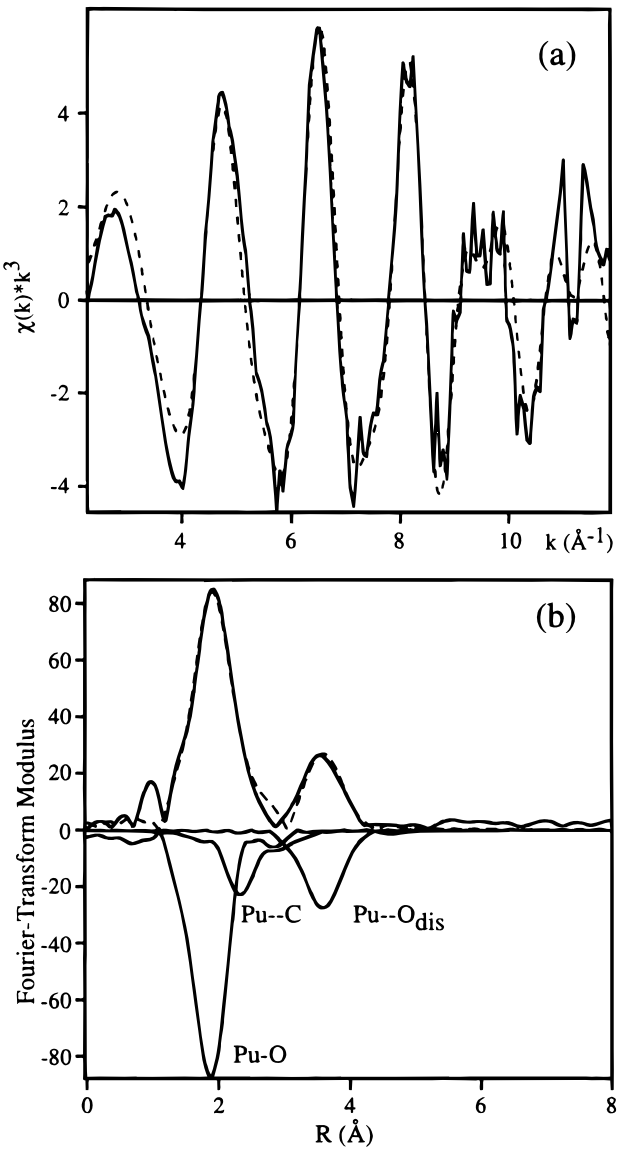

Figure 3. (a) Background-subtracted k^3-weighted EXAFS spectra (solid line) and fit (dashed line) of the limiting Pu(IV) complex in 2.5 M Na_2CO_3 solution. (b) Fourier tranforms without phase corrections of the k^3-weighted EXAFS spectra of the limiting Pu(IV) complex in 2.5 M Na_2CO_3 solution ($R = 0-8$ Å). The solid line is the experimental data, and the dashed line is the theoretical fit. Shown with negative FT amplitudes are the single shell contributions to the fit.

Table 3. Summary of k^3-Weighted EXAFS Structural Results for a $[Pu(CO_3)_5]^{6-}$ Solution[a]

bond	R (Å)	n	σ^2 (Å^2)
Pu−O	2.42(1)	10.0 (1.2)	0.0067(7)
Pu- - -C	2.88(2)	5.0 (0.6)	0.0043(11)
Pu- - -O	4.16(2)	5.0 (0.6)	0.0047(8)

[a] $\Delta E_0 = -4.5$ (1.2) eV, $S_0^2 = 0.85$, uncertainties reflect 2σ.

the number of atoms in the particular shell. Qualitatively, the intensity of the shells in the RDF spectra for $[Pu(CO_3)_n]^{4-2n}$ is significantly smaller than $[Pu(NO_3)_6]^{2-}$, consistent with a coordination number $n < 12$. After correcting the RDF intensity for differences in the bond distances of the ligands using the $1/r^2$ relationship, a quantitative analysis of the two oxygen-containing shells was performed. This analysis revealed average maximum values of 46.5(1.9) and 29.4(3.3), respectively, for $[Pu(NO_3)_6]^{2-}$, compared to 39.3 and 23.9 found for $[Pu(CO_3)_n]^{4-2n}$. The calculated ratios of the intensities, 0.846 and 0.813, respectively, imply that the number of carbonate ligands around the Pu(IV) core is indeed five ($^5/_6 = 0.833$), confirming the original best fit of $n = 10$.

Table 4. Summary of k^3-Weighted EXAFS Structural Results for the Four $[Pu(NO_3)_6]^{2-}$ Data Sets[31,37] and $[Pu(CO_3)_n]^{4-2n}$ Both Fit to $k = 3-11$

parameter	$[Pu(NO_3)_6]^{2-}$				$[Pu(CO_3)_n]^{4-2n}$
Pu−O, n	11.9	11.1	10.6	13.1	10.5
Pu−O, r (Å)	2.50	2.51	2.46	2.49	2.44
Pu−O, σ	0.099	0.100	0.090	0.099	0.101
Pu−O_{dis}, n	5.8	5.45	8.16	5.71	6.0
Pu−O_{dis}, r (Å)	4.17	4.18	4.17	4.17	4.15
Pu−O_{dis}, σ	0.085	0.083	0.099	0.077	0.100
fit error (RMS)	0.437	0.479	0.590	0.549	0.435

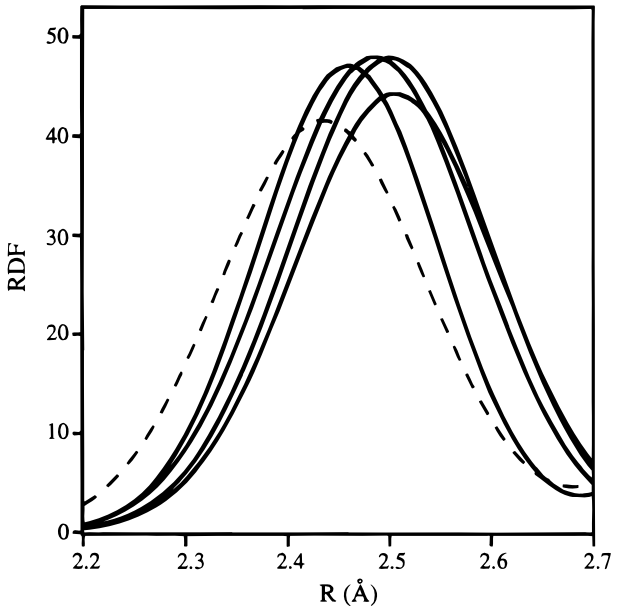

Figure 4. Radial distribution function, RDF, of the first shell of the fit waves for four different samples of $[Pu(NO_3)_6]^{2-}$ (solid lines) and $[Pu(CO_3)_n]^{4-2n}$ (dashed line).

The three single-shell contributions to the total EXAFS fit are shown with negative fit amplitudes in Figure 3b. The close spacing of Pu−O and Pu- - -C shells generates the appearance of a single peak in the EXAFS Fourier transform, and this feature is typical of actinide carbonate EXAFS data.[33,38] Despite its further distance from the Pu atom, the nonbonding distal O shell of the carbonate ligand derives its intensity from multiple scattering effects which are important when atoms are arranged in an approximately collinear fashion.[39] In such cases, the photoelectron is strongly focused by the intervening atom, resulting in significant amplitude enhancement. The focusing effect occurs for bidentate carbonate ligands, where Pu, C, and the distal O atom are all collinear. We find no evidence of a Pu- - -Pu backscattering interaction expected for polymeric species, consistent with maintenance of a monomeric species in solution. Similarly, we find no evidence for a Pu−O shell with a short Pu−O distance in the range 2.15−2.30 Å that would be expected for an OH^- ligand on an actinide center.[40] In addition, the combination of Pu−O, Pu- - -C, and distal Pu- - -O distances of 2.41, 2.88, and 4.16 Å is consistent with

(38) Clark, D. L.; Conradson, S. D.; Ekberg, S. A.; Hess, N. J.; Neu, M. P.; Palmer, P. D.; Tait, C. D. *J. Am. Chem. Soc.* **1996**, *118*, 2089.
(39) Teo, B. K. *EXAFS: Basic principles and data analysis*; Springer-Verlag: Berlin, 1986.
(40) Clark, D. L.; Conradson, S. D.; Neu, M. P.; Palmer, P. D.; Runde, W.; Tait, C. D. *J. Am. Chem. Soc.* **1997**, *119*, 5259.

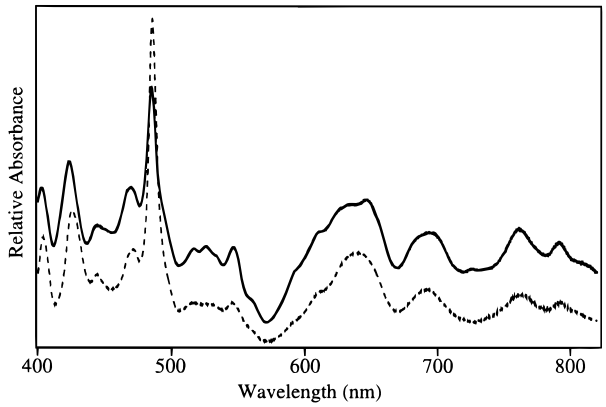

Figure 5. Electronic absorption spectrum of the limiting Pu(IV) species in high carbonate concentration (solid line; [Pu] = 0.1 M, $[CO_3^{2-}]$ = 2.5 M, 1 cm path length cell) and the diffuse reflectance spectrum of a single crystal of $[Na_6Pu(CO_3)_5]_2 \cdot Na_2CO_3 \cdot 33H_2O$ ground to a fine powder (dashed line).

bidentate carbonate ligation. A monodentate carbonate ligand would have a much longer Pu- - -C distance, on the order of 3.5 Å.[2] The combination of coordination numbers and bond distances provides a convincing argument for the existence of a monomeric $[Pu(CO_3)_5]^{6-}$ ion with bidentate carbonate ligation in 2.5 M Na_2CO_3 solution.

Electronic Absorption and Reflectance Spectroscopy. The room-temperature electronic absorption spectrum of the limiting Pu(IV) species recorded in 2.5 M Na_2CO_3 solution from 800 to 400 nm is shown in Figure 5. The absorption spectrum shows a manifold of weak ($\epsilon = 15-60$ $M^{-1}cm^{-1}$) absorption bands in the visible region (800−400 nm) consistent with Laporte-forbidden f → f transitions of the plutonium(IV) center. This spectrum is well-known, has been reported by many investigators,[6,8−11] and represents the fingerprint spectroscopic signature for the limiting Pu(IV) carbonato complex in solution. When the pH or carbonate concentration are changed enough to affect the speciation in solution, the absorption spectrum undergoes significant changes as new solution species are formed.[6,8,9,11] These spectroscopic changes have been shown by Capdevila,[9] Eiswirth,[8] and Hobart.[11] Therefore, the different absorbing Pu(IV) species are unique chromophores with their own spectroscopic fingerprint. Since single crystals of $[Na_6Pu(CO_3)_5]_2 \cdot Na_2CO_3 \cdot 33H_2O$ contain the $[Pu(CO_3)_5]^{6-}$ anion, we sought to determine the fingerprint electronic spectrum of the $[Pu(CO_3)_5]^{6-}$ chromophore using diffuse reflectance spectroscopy. The diffuse reflectance electronic spectrum of a single crystal of $[Na_6Pu(CO_3)_5]_2 \cdot Na_2CO_3 \cdot 33H_2O$ ground into a powder is shown in Figure 5 and is compared to the solution absorption spectrum of the limiting Pu(IV) carbonato complex in 2.5 M Na_2CO_3 solution in the 800−400 nm region. The peak-by-peak correspondence by position and relative absorption strengths is striking. Clearly, the Pu(IV) chromophore is the same in both cases, and the comparison confirms that the $[Pu(CO_3)_5]^{6-}$ ion is the limiting species in high carbonate solutions.

Concluding Remarks

The identification of the limiting complex in the Pu(IV) carbonate system under high carbonate concentration has been debated for over a decade.[2,3,6−13] By using a combination of single-crystal X-ray diffraction, solution EXAFS, and electronic absorption and diffuse reflectance spectroscopies, we have conclusively shown that the limiting complex is the $[Pu(CO_3)_5]^{6-}$ ion both in the solid state and in solution. This observation supports the assumption of the limiting species made by Capdevila et al.[9] during their recent studies. However, the identification of the limiting complex as $[Pu(CO_3)_5]^{6-}$ does not rule out the existence of mixed hydroxo−carbonato complexes under conditions of lower carbonate concentration, pH, or ionic strength. Indeed, the analogy with the Th system is intriguing. The data of Östhols et al.[22] are consistent with the presence of a limiting $[Th(CO_3)_5]^{6-}$ complex in equilibrium with $[Th(OH)_3(CO_3)]^-$ at lower carbonate concentrations. This result was recently confirmed by Felmy et al.[23] Similar structural studies to determine the identity of the other species in the Pu(IV) carbonate system of importance to nuclear waste isolation and disposal programs are currently in progress.

Experimental Section.

General Considerations. All operations were carried out inside HEPA-filtered fume hoods or negative-pressure gloveboxes designed for containment of radioactive materials. Standard radiochemical procedures were used throughout. A stock solution of 0.58 M ^{242}Pu(IV) in HCl solution served as our plutonium source. The Pu stock was made by first dissolving pure $^{242}PuO_2$ powder (99.93% ^{242}Pu) in concentrated $HClO_4$ with a few drops of 5% HF in HNO_3 to aid in dissolution. After all solid was dissolved, the solution was heated to fuming in order to oxidize all Pu to the VI state. The oxidation state was then adjusted to Pu(III) by reduction with hydrazine dihydrochloride and then oxidized to Pu(IV) using $NaNO_2$.[41] The resultant Pu(IV) was further purified by ion exchange chromatography. An equal volume of concentrated HNO_3 was added to the Pu(IV) solution and loaded on an anion exchange resin (Lewatit-9). Impurities were washed through by multiple additions of 8 M HNO_3 and washed with 9 M HCl to remove NO_3^-, and the purified Pu(IV) eluted with 0.5 M HCl. The resulting Pu(IV) was analyzed spectrophotometrically using the 470 nm absorption, $\epsilon = 56.5$ M^{-1} cm^{-1}.

The solution electronic absorption measurements were obtained in quartz cells on a Perkin-Elmer Lambda 19 or Cary model 5 spectrophotometer. Complete spectra in the range from 400 to 1000 nm as well as absorbance values at selected wavelengths were obtained. Measurements were made at 23 ± 1 °C.

The diffuse reflectance spectrum was recorded on a Perkin-Elmer Lambda 19 equipped with a 60 mm integrating sphere, and using the Kubelka−Munk transform to derive the "absorption" spectrum. The solid was ground to a fine powder in a glovebox and held in place in a quartz cell with a Teflon plunger. A protective Parafilm layer was peeled off upon removing the loaded cell from the glovebox, and a final Parafilm seal was applied to the back of the cell so that the resulting cell showed no external radioactive contamination. A background spectrum was determined using a quartz cell with a Teflon plunger covered with an Al_2O_3 TLC plate (no indicator).

The EXAFS sample cells were designed to enable EXAFS studies of radioactive ^{242}Pu at a nonnuclear facility. The primary sample cell consisted of a Teflon body with a Kapton (high-strength polyimide film, DuPont) window which had been pressure tested to 28.8 psi. The sample was loaded and tested for contamination and placed inside a secondary container of the same design, which was subsequently placed inside a third container with Kapton windows and mounted inside the X-ray experimental hutch. The experimental hutch was modified for radiochemical experiments by using a portable experimental enclosure within the hutch. This allowed for maintenance of three zones of negative pressure, and the vacuum system passed through 0.3 μ HEPA filters. The hutch was equipped with continuous air monitors and radiation sampling safety equipment and monitored continuously throughout the course of experiment.

EXAFS Data Acquisition and Analysis. Plutonium L_{III} edge X-ray absorption spectra were collected at the Stanford Synchrotron Radiation Laboratory on wiggler beamline 4−2 (unfocused) with an electron beam

(41) Newton, T. W.; Hobart, D. E.; Palmer, P. D. *The preparation and stability of pure oxidation states of neptunium, plutonium, and americium*; Report LA-UR-86-967; Los Alamos National Laboratory: Los Alamos, NM, 1986.

energy of 3.0 GeV and maximum stored beam currents between 60 and 100 mA. A Si (220) double-crystal monochromator was used. Rejection of higher harmonic content in the X-ray beam was achieved by employing a flat Rh-coated quartz mirror tuned at a critical angle to reject photons having energies above 24 000 eV. Having rejected greater than 95% of the higher order harmonics with the mirror, the monochromator was operated fully tuned with respect to θ, the orientation between the two crystals. Spectra were collected simultaneously both in transmission mode using three N_2-filled ionization chamber detectors, and in fluorescence mode using a 13-element Ge detector (Canberra). For the Ge detector, the count rate was controlled by adjusting the hutch entrance slits or by moving the detector closer to, or farther from, the sample windows. Under these conditions, no dead-time correction was necessary. Data reduction and analysis were performed using techniques described elsewhere.[42] The summed data for each detector (transmission or fluorescence) were then inspected, and only those channels that gave high-quality signal-to-noise ratios were included in the final weighted average. Three EXAFS scans were collected on the solution at ambient temperature (ca. 25 °C). The spectra were energy calibrated by simultaneously measuring the spectrum of a Zr foil placed between the second and third ion chambers, defining the first inflection point at the Zr K edge as 17 999.35 eV. In any series of scans, the measured energy of the first inflection of the Zr foil spectrum varied by less than 1 eV. Averaged EXAFS data were referenced to the Zr calibration of the first scan of a series, since the energy drift in any series of scans was too small to perturb the EXAFS oscillations. The data were manipulated and analyzed using the WinXAS 97 package.[43] The data were normalized by setting the edge jump equal to unity above the ionization threshold ($k = 0$), defined as 18 064 eV. A five-region cubic spline function was used to fit the background over the EXAFS region which extended out to $k = 11.864$ Å^{-1}. Fourier transforms of the k^3-weighted data were calculated over the range $k = 2.288-11.864$ Å^{-1} with a Gaussian window parameter of 30. Theoretical phases and amplitudes were derived from the program FEFF7[44,45] to fit the contributions from the O and C neighbors. For the distal O shell, the single path as well as two multiple scattering paths, one three-legged and one four-legged, were included in the analysis. The parameters refined in the fit were ΔE_0, the photoelectron energy threshold; R_i, the distance from Pu to atom i; n_i the number of i atoms; and σ_i, the DW term for atom i. The coordination numbers for the C shell and the distal O shell were correlated to be half the coordination number of the first O shell as required by the stoichiometry of a bidentate carbonate ligand. The quality of the fit was determined by the residuum between the fit and k space data.

X-ray Crystallography. A dark green, parallelepiped-shaped crystal was thinly coated with epoxy and placed in a quartz capillary. The capillary was then coated with a thin film of acrylic dissolved in ethyl acetate (Hard as Nails nail polish). (*Note: This triple containment was necessitated by the associated health hazards of transuranic materials.*) Data were collected on a Siemens P4/PC diffractometer. The radiation used was graphite-monochromated Mo Kα radiation ($\lambda = 0.710\ 73$ Å). The lattice parameters were optimized from a least-squares calculation on 25 carefully centered reflections of high Bragg angle. The data were collected using ω scans with a 1.0° scan range. Three check reflections monitored every 97 reflections showed a 50% decay of the crystal over the course of the data collection. Due to high initial crystal quality the intensity at the end of the data collection was still adequate. Lattice determination and data collection were carried out using XSCANS Version 2.10b software. All data reduction, including Lorentz and polarization corrections, structure solution, and graphics, were performed using SHELXTL PC Version 4.2/360 software.[46] The structure refinement was performed using SHELXL-93 software.[47] The data were corrected for absorption using the ellipsoid option in the XEMP facility of SHELXTL PC. Data collection parameters are given in Table 1.

The structure was solved in space group $P2_1/c$ using Patterson techniques. This solution yielded the plutonium and sodium atoms. Subsequent Fourier synthesis gave the remaining light atom positions. A lattice carbonate ion was found very close to an inversion center and was subsequently modeled as a partial occupancy carbonate ion (Figure 2). No hydrogen atoms were fixed or refined due to the inability to locate the hydrogens of the terminal water molecules. The final refinement included anisotropic thermal parameters on all atoms and converged to $R_1 = 0.0337$ and $wR_2 = 0.0775$, where $R_1 = \sigma||F_o|-|F_c||/\sigma|F_o|$; $wR_2 = [\sum[w(F_o^2 - F_c^2)^2]/\sum[w(F_o^2)^2]]^{1/2}$, and $w = 1/[\sigma^2(F_o^2) + (0.0397P)^2 + 5.0273P]$.

Acknowledgment. We thank Drs. T.W. Newton, M. P. Neu, and W. Runde for helpful discussions. This research was supported by the Nuclear Material Stabilization Task Group, and by the U.S. DOE Office of Basic Energy Sciences, under Contract No. W-7405-ENG-36 with the University of California. XAS experiments were performed at the Stanford Synchrotron Radiation Laboratory, which is supported by the U.S. DOE Office of Basic Energy Sciences.

Supporting Information Available: An X-ray crystallographic file, in CIF format, for the structure determination of $[Na_6Pu(CO_3)_5]_2 \cdot Na_2CO_3 \cdot 33H_2O$ is available on the Internet only. Access information is given on any current masthead page.

IC971190Q

(42) Prins, R.; Koningsberger, D. C. *X-ray absorption: Principles, applications, techniques for EXAFS, SEXAFS, and XANES*; Wiley: New York, 1988.
(43) Ressler, T. *J. Phys. IV* **1997**, *7*, C2.
(44) Rehr, J. J.; Mustre-de-Leon, J.; Zabinsky, S. I.; Albers, R. C. *J. Am. Chem. Soc.* **1991**, *113*, 5135.
(45) Mustre-de-Leon, J.; Rehr, J. J.; Zabinsky, S. I.; Albers, R. C. *Phys. Rev. B* **1991**, *44*, 4146.
(46) XSCANS and SHELXTL PC are products of Siemens Analytical X-ray Instruments, I., 6300 Enterprise Lane, Madison, WI 53719.
(47) Sheldrick, G. M. *SHELXL-93*; University of Göttingen: Germany, 1993.